

Catalytic oxidation mechanism of methane via transition metals Pt, Pd and Ag

Jun Zhang*, Tingting Hu, Li Wang & Chuan Dong

Institute of Environmental Science, Shanxi University, Taiyuan 030006, PR China

Email: dc104@sxu.edu.cn

Received 13 February 2018; revised and accepted 20 November 2018

The mechanisms for catalytic oxidation of methane via transition metals Pd, Pt and Ag in gas phase have been theoretically investigated using density functional theory (DFT). The results reveal similar pathways of C-H activation via Pd, Pt with the formation of atom-molecule complex, transition state and product. Catalytic oxidation using Pd and Pt exhibited different reaction energies. The possible pathway of C-H activation via Ag has been proposed. First, the abstraction of H from CH₄ by Ag occurs followed by the dissociation of CH₃ and AgH. With the calculation of energy parameters and rate constants, the order of catalytic performance of the three transition metals has been found to be Pt>Pd>Ag. A theoretical foundation for the catalytic oxidation of methane by single active atoms has been established.

Keywords: Methane, Catalytic oxidation, Transition metals, Density functional theory, C-H activation

Methane is a cheap and high-quality fuel gas. The search for efficient catalysts for methane oxidation remains a challenging task. As a key step to achieve methane transformation, C-H activation is of high interest¹⁻⁴. It is an established fact that it is possible to activate the C-H bond in CH₄ by transition metals. The empty *d* orbital of metal atom accepts the electrons from the bonding σ orbital of C-H bond, while the filled *d* orbital of metal atom donates electrons to the antibonding σ^* orbital of C-H bond. The C-H bond is weakened or broken by the donation or acceptance of electron⁵.

The catalytic oxidation of methane has been a research hotspot for a long time⁶⁻¹⁰. Currently, it is still difficult to confirm the reaction mechanism experimentally due to the complexity of catalytic reaction as well as the short-lived and/or low concentration of intermediates. To clarify the reaction mechanism, quantum chemical calculations have been applied to generate information about the structure and energy of the intermediate and transition state¹¹⁻¹³. Some theoretical investigations on the catalytic oxidation of methane via Pd, Pt and Ag¹⁴⁻¹⁶ have been reported by using the ideal crystal surface models¹⁷. However, it is still impractical to apply high-level quantum chemical method to study a complicated system. In addition, it becomes unreliable for the comparison of mechanism among metals based on their individual data from different computation systems.

Density functional theory (DFT) has been proved to be reliable for the geometric optimization of systems, calculation of potential energy surface, electronic

structure and thermodynamic calculations, hence it is widely used in the study of catalytic oxidation of methane¹⁸⁻²⁰. B3-based DFT procedures provide an efficient means of determining harmonic vibrational frequencies and derived thermochemical quantities. PBE is preferred in the calculation of weak interaction over traditional functionals as well²¹.

The single atom catalyst is highly active, selective and stable, and has shown great potential in its application to methane catalytic oxidation²². In gas-phase experiments the difficult-to-control or poorly defined parameters in real-life metal-based catalytic usage can be excluded. In this work, the microscopic mechanism of C-H activation in CH₄ using Pd, Pt and Ag in gas phase were investigated using DFT methods. A theoretical foundation was provided for the catalytic oxidation of methane by gas-phase or cluster-confined single active atoms. The catalytic performances of the transition metals were evaluated along with the suggested activation mechanisms.

Materials and Methods

The DFT calculations were made using Gaussian 03 quantum chemistry software²³. The structures and energy information of reactants, transition states, intermediates and products in the catalytic activation of CH₄ via Pd, Pt and Ag were obtained employing three methods viz., B3LYP²⁴, B3PW91²⁵ and PBE/PBE²⁶ respectively. The vibration frequencies at each point along the reaction pathway were also calculated. As one of the most widely used ECP

(effective core potential) basis sets, LanL2DZ is widely used in calculations pertaining to transition metal systems. Here, LanL2DZ basis set was selected to accurately deal with the outer electrons of Pd($4s^2 4p^6 4d^{10}$), Pt($5s^2 5p^6 5d^9 6s^1$) and Ag($4s^2 4p^6 4d^{10} 5s^1$), while their core electrons were treated in the approximation of frozen core. The 6-311G (d, p) basis set was performed for C and H. No significant spin contamination was found in the calculations.

Results and Discussion

In the catalytic oxidation of methane, the key role of Pd is to activate the C-H bond in CH_4 . The oxidation is facilitated with the generation of CH_3PdH . The main structure diagram and symmetry in the C-H activation are illustrated in Fig. 1.

Three issues were addressed in the calculation: the reaction pathway, variation trend in geometric configuration and the stationary-point energy in potential-energy curve. The geometry parameters of all structures in Fig. 1 were calculated by three DFT methods and energy changes for activation were also noted. The results from the three DFT methods were consistent with each other, and also in agreement with literature¹⁴. Therefore, the B3LYP data have been representatively used in the following discussion.

Upon the interaction of Pd and CH_4 , a relatively stable atom-molecule complex (RC) with C_{2v}

symmetry is generated with a binding energy of 5.9 kcal/mol. The bond lengths of C-H(1) and C-H(3) (two C-Hs toward Pd) are slightly elongated from 1.090 Å to 1.111 Å, while the Pd-C bond length is 2.482 Å (Supplementary Data, Tables S1-S2).

With activation, the bond length of C-H(1) is elongated to 1.663 Å while the bond length of Pd-C is shortened to 2.091 Å. The transition state (TS) under C_s symmetry is formed with activation energy of 13.4 kcal/mol. With the activation of Pd, TS oscillates between the cleavage and formation of C-H(1). The TS is also validated by the unique imaginary frequency of 789i in frequency calculation.

Finally, the product (P) under C_s symmetry is formed via TS. The bond length of Pd-C is shortened to 2.011 Å, and the bond length of C-H(1) is elongated to 2.406 Å for the product. The energy change from RC to product P amounts to 8.6 kcal/mol. This value is equivalent to that of the cleavage energy of C-H with the activation of Pd, which is lower than the bond energy of C-H in CH_4 (104.9 kcal/mol). This indicates that Pd has a fairly high catalytic activity.

The main changes of electron density in HOMO and LUMO along the reaction pathway is shown in Fig. 2. When Pd approaches towards CH_4 , a RC is generated. The combination of CH_4 with Pd is

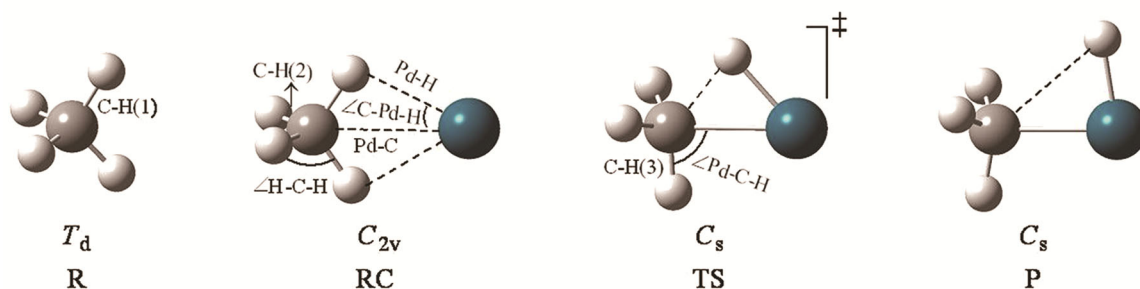


Fig. 1 — Structures and point group symmetries of stationary points along the reaction coordinate for C-H activation of CH_4 via Pd.

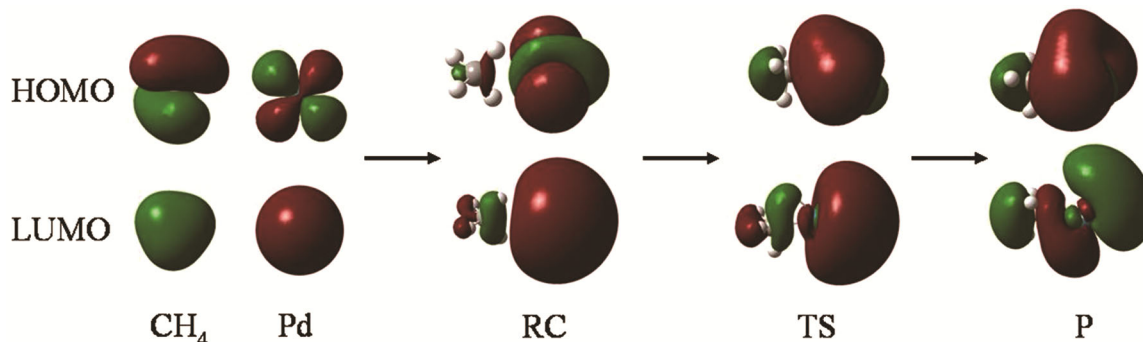


Fig. 2 — The molecular orbital (HOMO, LUMO) diagram of the stationary points along the reaction coordinate for C-H activation of CH_4 via Pd.

evidenced from the electron cloud of HOMO and LUMO. When TS is formed, the bonding and anti-bonding orbitals of C-H overlap with the hybridized d orbital of Pd. It suggests that the empty d orbital of Pd accepts electrons from the C-H bonding orbital σ , while the filled d orbital of Pd donates electrons to the C-H anti-bonding orbital σ^* . When product P is formed, the C-H bonds are completely broken. The electron density near Pd in HOMO orbit shows a distinct increase.

Pt plays the same role as that of Pd in the catalytic oxidation of methane i.e., the C-H activation by Pt gives CH_3PtH . The structural diagram and corresponding symmetry are depicted in Fig. 3. The corresponding geometric parameters were calculated using the B3LYP method. The energy changes in the whole reaction process were also recorded. The potential-energy curve in Fig. 4 is plotted through scanning at fixed Pt-C length. These data are consistent with literature¹⁵.

The difference in C-H activation by Pt and Pd is shown in Fig. 4. There are two low-energy states of Pt, the triplet (d^9s^1 , 3D_3) and singlet (d^{10} , 1S_0) in the reaction. When Pt interacts with CH_4 , a RC with C_{2v}

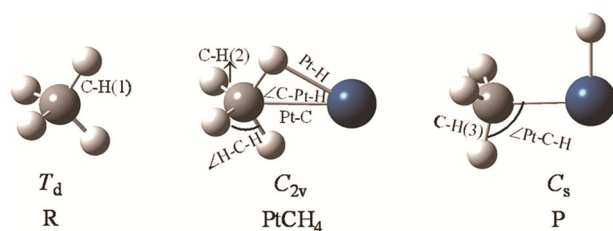


Fig. 3 — Structures and point group symmetries of the stationary points along the reaction coordinate for the C-H bond activation of CH_4 via Pt.

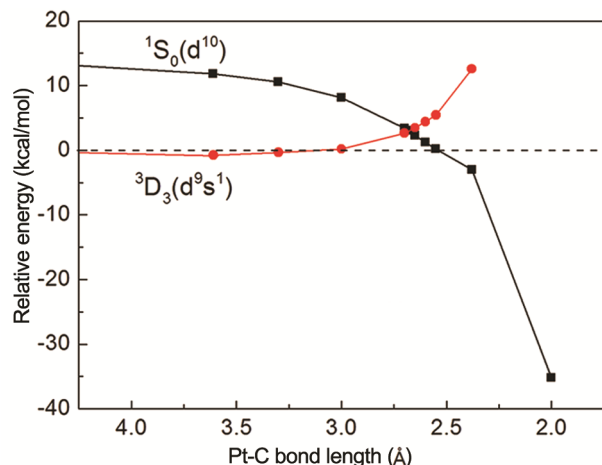


Fig. 4 — Potential energy curves for the C-H activation of CH_4 via triplet Pt (d^9s^1 , 3D_3) and singlet Pt (d^{10} , 1S_0).

symmetry is formed. The triplet $\text{Pt}(^3D)$ and CH_4 are bound at a Pt-C length of 3.61 Å, with a binding energy of -0.8 kcal/mol. The bond lengths of C-H(1) and C-H(3) in RC are stretched a little from 1.090 Å to 1.092 Å. This indicates that the binding of $\text{Pt}(^3D)$ with CH_4 is very weak at the beginning. The Pt-C length decreases with increase in binding energy (Supplementary Data, Table S3-S4).

On the other hand, the RC under C_{2v} symmetry can also be generated from the combination of triplet $\text{Pt}(^1S)$ with CH_4 . In this case, with the decrease of Pt-C length, the binding energy decreases gradually. It is noteworthy that the potential energy curves of triplet state and singlet state are intersected at a point, where the Pt-C length is 2.685 Å. At this point, the energy of $\text{Pt}(^1S)\text{CH}_4$ and $\text{Pt}(^3D)\text{CH}_4$ are approximately equivalent although their structures are slightly different. The energy of $\text{Pt}(^1S)\text{CH}_4$ is about 2.8 kcal/mol higher than that of the triplet state reactant $\text{Pt}(^3D)+\text{CH}_4$. Therefore, the complex indicated at the intersection point is determined to be the TS with the unique imaginary frequency of 382i. Thereafter, the singlet state product $\text{HPt}(^1S)\text{CH}_3$ under C_s symmetry is generated from TS. For the product, the Pt-C length contracts to 2.00 Å, and the C-H(1) bond length elongates to 2.593 Å.

Thus, CH_4 is activated with the ground state $\text{Pt}(d^9s^1)$ and low energy state $\text{Pt}(d^{10})$ together. The activation energy for the reaction is 3.6 kcal/mol, and the released energy is 34.4 kcal/mol. Pt performs comparatively better than Pd in the catalytic oxidation of methane.

The outer-shell electron configuration of $\text{Ag}(4d^{10}5s^1)$ is significantly different from $\text{Pd}(4d^{10})$ or $\text{Pt}(4d^95s^1)$. Therefore, Ag follows a reaction pathway different from Pd or Pt. The geometry parameters and energy values were recorded accordingly. The calculation indicates that there are two possible Ag reaction pathways in the C-H activation reaction (Fig. 5).

In one pathway, the RC under C_{2v} symmetry is formed with a binding energy of -0.1 kcal/mol. The bond length of C-H(1) and C-H(3) are slightly elongated from 1.090 Å to 1.091 Å. This suggests that the interaction between Ag and CH_4 is very weak. The product P(HAgCH_3) is finally formed via the TS with C_s symmetry. In this pathway, the activation energy is 60.1 kcal/mol, and the absorbed energy is 42.5 kcal/mol (Supplementary Data, Table S5-S6). For the other pathway, the H of CH_4 is associated with Ag, and then the products CH_3 and AgH are

formed through direct dissociation. As the reaction proceeds, the C-H(1) bond length is elongated, while the Ag-H bond length is shortened. The total absorbed energy in the reaction is 52.1 kcal/mol, which is lower than the C-H bond energy of 104.9 kcal/mol in CH₄. This indicates that the C-H bond cleavage is indeed activated by Ag. This result is consistent with the reports that Ag helps to improve the coke resistance and catalyst activation in methane dissociation²⁷ and is also of potential practical interest to both the C-H bond activation and subsequent ethylene release processes by the cooperative action of multiple molecules adsorbed on clusters²⁸.

In addition, the absorbed energy in the two pathways activated by Ag, is higher than that of Pd (8.6 kcal/mol), suggesting the poorer catalytic performance of Ag than that of Pd. Thus, the catalytic performance is ranked in the order Pt>Pd>Ag for the C-H activation of CH₄ based on the required energy.

The prediction of the chemical reaction rate constant is among the challenges encountered in the field of theoretical chemistry calculation²⁹. The kinetic method is used to study the information about reaction path and rate constant of reaction, which reveals the microscopic mechanism of the reaction. The catalytic performance of Pt, Pd and Ag was

assessed by the comparison of three parameters: enthalpy change, Gibbs free energy change and the rate constant (298 K, 1atm) of the reaction. As listed in Table 1, $\Delta G^\circ < 0$ and $\Delta H^\circ < 0$ occurs only for Pt catalyzed C-H activation. It suggests that C-H activation is more tenable via Pt than the other two transition metals.

Assuming that 1 mol molecules participated in the reaction, eqn 1 (details of derivation are provided as Supplementary Data) is employed in the following calculation of rate constant³⁰:

$$k = \frac{RT}{h} \exp\left(\frac{\Delta S^{\ddagger}}{R}\right) \exp\left(-\frac{\Delta H^{\ddagger}}{RT}\right) \quad \dots (1)$$

The rate constant of each reaction in Table 1 has been calculated by incorporating the values of reaction barrier H^{\ddagger} , entropy change S^{\ddagger} and Planck's constant $h = 6.626 \times 10^{-34}$ J s in the above equation. Overall, the catalytic performance order Pt>Pd>Ag is confirmed again by the rate constants. This is consistent with the DFT results. For Ag catalyzed C-H activation, the rate constant was used to determine the better pathway. The H of CH₄ first associates with Ag, forming a RC complex, and then the RC complex directly dissociates into CH₃ and AgH.

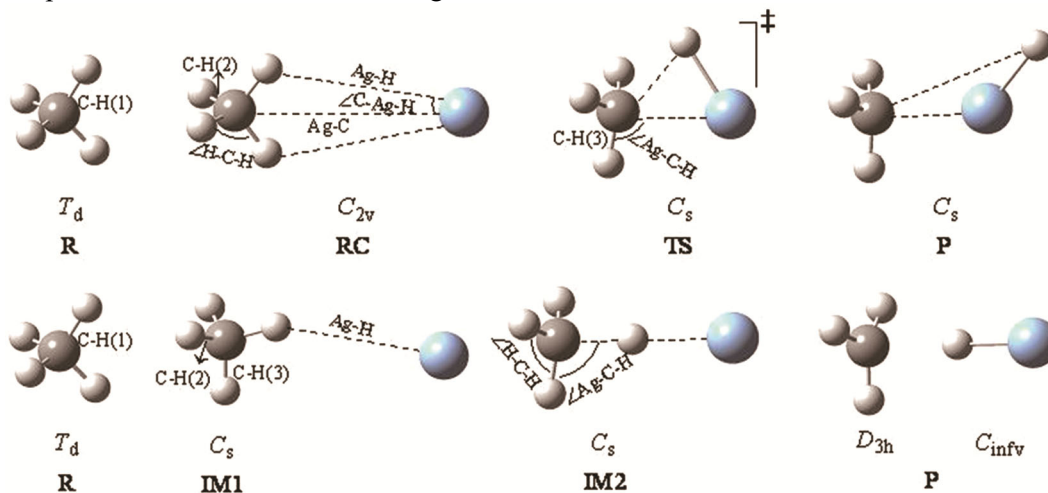


Fig. 5 — Structures and point group symmetries of the stationary points along the two reaction coordinates for the C-H activation of CH₄ via Ag.

Table 1 — Enthalpy, Gibbs free energy, reaction barrier, entropy and rate constant values of the C-H activation in CH₄ via Pd, Pt and Ag, at 1atm and 298 K

Reactions	ΔH° (kcal mol ⁻¹)	ΔG° (kcal mol ⁻¹)	ΔH^{\ddagger} (kcal mol ⁻¹)	ΔS^{\ddagger} (kcal mol ⁻¹ K ⁻¹)	K (s ⁻¹)
Pd+CH ₄ →CH ₃ PdH	8.1	9.3	12.9	-0.0038	1.91×10 ²⁶
Pt+CH ₄ →CH ₃ PtH	-34.7	-32.6	2.9	-0.0077	5.81×10 ³²
Ag+CH ₄ →CH ₃ AgH	43.2	43	59.9	-0.0048	3.89×10 ⁻⁹
Ag+CH ₄ →CH ₃ +AgH	53.8	45.9	53.8	0.0263	7.27×10 ²

Conclusions

Pd and Pt have similar reaction pathways for C-H activation in CH₄. The RC is firstly generated, and then the product is formed via TS. However, the difference in energy is large between Pd and Pt catalysis. The activation energy of CH₄ in Pd catalysis is 13.4 kcal/mol, and the total absorbed energy is about 8.6 kcal/mol. The potential energy curves of the two low-energy states show that Pt intersects at the point where the Pt-C length is 2.685 Å. The activation energy of Pt catalysis is 3.6 kcal/mol and the released energy is 34.4 kcal/mol in the reaction.

There are two possible reaction pathways for the C-H activation of CH₄ via Ag. From the rate constants and energy change, the possible pathway involves the initial association of Ag and H in CH₄, and then the direct dissociation into CH₃ and AgH. The absorbed energy of the reaction is 52.1 kcal/mol. Comparing the activation energy, enthalpy change and rate constant, the catalytic performance is ranked in the order Pt>Pd>Ag. The present work is an important contribution in the study of the mechanism of gas phase C-H activation or cluster-confined single active atoms. It provides a theoretical basis for the catalytic oxidation of methane with high quality and efficiency.

Supplementary Data

Supplementary Data associated with this article are available in the electronic form at [http://www.niscair.res.in/jinfo/ijca/IJCA_57A\(12\)1443-1447_SupplData.pdf](http://www.niscair.res.in/jinfo/ijca/IJCA_57A(12)1443-1447_SupplData.pdf).

Acknowledgement

This work was supported by grants from the National Natural Science Foundation of China (No. 21575084), the Nature Science Foundation of Shanxi Province of China (No. 201601D102009), the Provincial Government for the Oversea Hundreds of talents Program (No. 205107001-2015), the Program of 131 Leading Principal Investigator (No. 205544901006-2015).

References

- 1 Labinger J A & Bercaw J E, *Nature*, 417 (2002) 507.
- 2 Li C, Dinoli C, Coel Y & Etienne M, *J Am Chem Soc*, 137 (2015) 12450.
- 3 Schröder D & Schwarz H, *Proc Natl Acad Sci USA*, 105 (2008) 18114.
- 4 Li H, Li B J & Shi Z J, *Catal Sci Technol*, 1 (2011) 191.
- 5 Vastine B A & Hall M B, *Coordin Chem Rev*, 253 (2009) 1202.
- 6 Sen A, Benvenuto M A, Lin M, Hutson A C & Basickes N, *J Am Chem Soc*, 116 (1994) 998.
- 7 Ketteler G, Ogletree D F, Bluhm H, Liu H, Hebenstreit E L & Salmeron M, *J Am Chem Soc*, 127 (2005) 18269.
- 8 Firth J G, *Trans Faraday Soc*, 62 (1966) 2566.
- 9 Kundakovic L & Flytzani-Stephanopoulos M, *Appl Catal A-Gen*, 183 (1999) 35.
- 10 Blomberg M R, Siegbahn P E & Svensson M, *J Am Chem Soc*, 114 (1992) 6095.
- 11 Fratesi G, Gava P & De Gironcoli S, *J Phys Chem C*, 111 (2007) 17015.
- 12 Dedieu A, *Chem Rev*, 100 (2000) 543.
- 13 Bagno A & Saielli G, *Phys Chem Chem Phys*, 13 (2011) 4285.
- 14 De Jong G T, Sola M, Visscher L & Bickelhaupt F M, *J Chem Phys*, 121 (2004) 9982.
- 15 Carroll J J, Weisshaar J C, Siegbahn P E, Wittborn C A & Blomberg M R, *J Phys Chem*, 99 (1995) 14388.
- 16 Yu J & Anderson A B, *J Am Chem Soc*, 112 (1990) 7218.
- 17 Liao M S, Au C T & Ng C F, *Chem Phys Lett*, 272 (1997) 445.
- 18 Jong G T D, Geerke D P, Diefenbach A & Bickelhaupt F M, *Chem Phys*, 313 (2005) 261.
- 19 Lü C, Ling K & Wang G, *Chinese J Catal*, 30 (2009) 1269.
- 20 Psfogiannakis G, St-Amant A & Ternan M, *J Phys Chem B*, 110 (2006) 24593.
- 21 And A P S & Radom L, *J Phys Chem*, 100 (1996) 16502.
- 22 Guo X, Fang G, Li G, Ma H, Fan H, Yu L, Ma C, Wu X, Deng D, Wei M, Tan D, Si R, Zhang S, Li J, Sun L, Tang Z, Pan X & Bao X, *Science*, 344 (2014) 616.
- 23 Frisch M J, Trucks G W & Schlegel H B: Gaussian 03, G03RevB.01. Gaussian, Inc, Pittsburgh PA (2003).
- 24 Lee C, Yang W & Parr R G, *Phys Rev B*, 37 (1988) 785.
- 25 Perdew J P, Chevary J A, Vosko S H, Jackson K A, Pederson M R, Singh D J & Fiolhais C, *Phys Rev B*, 46 (1992) 6671.
- 26 Perdew J P, Burke K & Ernzerhof M, *Phys Rev Lett*, 77 (1996) 3865.
- 27 Xu Y, Li P, Fan C, Zhou X & Zhu Y, *China Science Paper Online*, 5 (2010) 12.
- 28 Lang S M, Bernhardt T M, Barnett R N & Landman U, *Angew Chem Int Ed*, 49 (2010) 980.
- 29 Smith I W M, *Kinetics and Dynamics of Elementary Gas Reactions Butterworths*, (Butterworths, London) 1980.
- 30 Prigogine I, *Chemical Kinetics and Dynamics*, (Prentice-Hall, New Jersey) 1989.